Analytica Chimica Acta 1153 (2021) 338283

Contents lists available at ScienceDirect

Analytica Chimica Acta

journal homepage: www.elsevier.com/locate/aca

Plasmonic TiO_2@Au NPs//CdS QDs photocurrent-direction switching system for ultrasensitive and selective photoelectrochemical biosensing with cathodic background signal

Ruiying Yang [a], Guihua Jiang [b], Jie Liu [a], Yilin Wang [a], Ningge Jian [a], Leiliang He [a], Li'e Liu [a], Lingbo Qu [c], Yongjun Wu [a, b, *]

[a] College of Public Health, Zhengzhou University, Zhengzhou, 450001, China
[b] College of Chemistry and Molecular Engineering, Zhengzhou University, Zhengzhou, 450001, China
[c] Institute of Green Catalysis, College of Chemistry, Zhengzhou University, Zhengzhou, 450001, China

HIGHLIGHTS

- >An ultrasensitive and selective photoelectrochemical biosensor was developed for the detection of carcinoembryonic antigen.
- >The innovative TiO_2@Au nanoparticles as the photoactive material showed a cathodic background signal.
- >The plasmonic TiO_2@Au nanoparticles//CdS quantum dots were photocurrent-direction switching system.

GRAPHICAL ABSTRACT

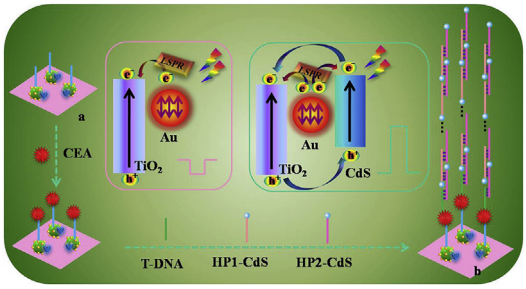

ARTICLE INFO

Article history:
Received 12 November 2020
Received in revised form
28 January 2021
Accepted 1 February 2021
Available online 7 February 2021

Keywords:
Photoelectrochemical biosensor
TiO_2@Au NPs//CdS QDs
LSPR effect
Photocurrent-direction switching
Cathodic background signal
CEA

ABSTRACT

An ultrasensitive and selective photoelectrochemical (PEC) biosensor with cathodic background signal was developed for the detection of carcinoembryonic antigen (CEA) based on innovative plasmonic TiO_2@Au nanoparticles//CdS quantum dots (TiO_2@Au NPs//CdS QDs) photocurrent-direction switching system, coupling with hybridization chain reaction (HCR) for the signal amplification. Firstly, innovative TiO_2@Au NPs were successfully fabricated through in situ ascorbic acid-reduction of Au NPs dispersed on TiO_2 surface, and TiO_2@Au NPs as the photoactive material showed a cathodic background signal. When target CEA existed, a sandwich-type reaction was performed in capture CEA aptamer-modified TiO_2@Au NPs and trigger CEA aptamer. Interestingly, after HCR triggered by target CEA, a mass of CdS QDs were introduced into the biosensing platform, resulting in the formation of TiO_2@Au NPs//CdS QDs system, along with the switch of photocurrents from cathodic to anodic. The obtained remarkable anodic photocurrent was depended on the localized surface plasmon resonance (LSPR) effect of Au between TiO_2 and CdS. Under the optimal conditions, plasmonic TiO_2@Au NPs//CdS QDs photocurrent-direction switching PEC biosensing platform with cathodic background signal exhibited ultrasensitive for the determination of CEA with a low limit of detection of 18.9 fg/mL. Importantly, the proposed PEC biosensor can eliminate the interferences of the initial photocurrent and background signal, and has high-efficiency anti-interference ability, satisfactory stability and excellent reproducibility, which may have great potentials in bioanalysis and disease diagnosis.

* Corresponding author. College of Public Health, Zhengzhou University, Zhengzhou, 450001, China.
E-mail address: wuyongjun135@126.com (Y. Wu).

https://doi.org/10.1016/j.aca.2021.338283
0003-2670/

1. Introduction

As an emerging and promising analytical technique for biomarkers detection, photoelectrochemical (PEC) biosensor has attracted extensive research owing to low background, cost effectiveness, simple operation, and easy miniaturization [1–8]. Notably, the properties of photoactive materials directly determine the PEC efficiency, will further influence the detection sensitivity in PEC biosensing system [9–13]. Nowadays, titanium dioxide (TiO_2), as a representative photoactive material, has received increasing attention for the construction of PEC biosensors because of its high electronic mobility good biocompatibility, inexpensiveness, and chemical stability [14–16]. However, one disadvantage of TiO_2 relies on the narrow light absorption regions, which can only use ultraviolet light as light source and limits its application [17–19]. To address this issue, plasmonic metallic were usually applied to modify TiO_2 [20–22]. Compare with the pure TiO_2, the nanocomposite showed strong absorption intensity in the visible region because of the strong localized surface plasmon resonance (LSPR) effect of plasmonic metallic. For example, a plasmonic enhancement coupling with defect-engineered TiO_{2-x} was reported for sensitive PEC biosensing [23]. A plasmonic PEC biosensor based on the cyclodextrin and Au—TiO_2 composite for prion assay was developed in our group [24]. Despite the above success, these Au—TiO_2 composites show anodic background signal and result in interference from some reductive components in complex biological samples. Therefore, it remains great challenging to seek new avenues to surmount the above phenomenon and owns enormous performance for anti-interference capability.

Carcinoembryonic antigen (CEA) is one of the widely used biomarkers for clinic diagnosis and treatment of cancer [25–27]. Massive clinical data showed when the level of CEA biomarker concentrations in serum, tissue, or saliva increases or decrease, they can be indicative of disease states [28–30]. Up to now, many efforts are devoted to the development of advanced PEC biosensing platforms for CEA assay. For example, Tang et al. developed a $NaYF_4$:Yb, Er upconversion nanotransducer with in-situ fabrication of Ag_2S for near-infrared light responsive PEC assay of CEA [31]. Ye et al. applied a PEC biosensor for CEA detection based on SnS_2-GR with multiple quenching effects of Au@CuS-GR [32]. In above literatures, when these biosensors added CEA, the photocurrent enhancer or quencher was imported to produce “signal-on” or “signal-off” response, thus the CEA was quantified. However, the single photocurrent direction is difficult to identify whether the signal response is produce by target object or distractors, resulting in false positive or negative errors. Recently, some PEC biosensors based on the photocurrent-direction switching systems (such as CdS//hemin, CdS//CdTe) have been developed in our group [33–35], where the switching system was formed after the addition of the target, achieving a reverse photocurrent. This fascinating experimental phenomena inspires us to establish novel PEC biosensors of CEA to overcome the above problems on initial photocurrent and background signal.

Herein, an ultrasensitive and selective PEC biosensor based on plasmonic TiO_2@Au NPs//CdS QDs photocurrent-direction switching system with cathodic background signal was for the first time constructed for CEA detection (Scheme 1A). Firstly, innovative TiO_2@Au NPs were successfully fabricated through in situ ascorbic acid (AA)-reduction of Au nanoparticles (NPs) dispersed on the surface of TiO_2 NPs different from traditional preparation methods [36–39]. Surprisely, it firstly found that TiO_2@Au NPs modified indium tin oxide (ITO) electrode showed cathodic background signal due to the LSPR effect coupling TiO_2 with Au NPs [40,41]. After the immobilization of capture CEA aptamer (C-DNA) via Au—S bond, CEA was added, and a sandwiched reaction was performed among the initially assembled C-DNA and trigger CEA aptamer (T-DNA). Afterwards, the T-DNA induced the formation of hybridization chain reaction (HCR) between CdS-labeled DNA probes to introduce large amounts of CdS quantum dots (QDs), and the plasmonic TiO_2@Au NPs//CdS QDs were formed, resulting in the photocurrent-direction switch from cathodic to anodic, due to the energy level match between TiO_2@Au and CdS. Based on the target-induced photocurrent-direction switching with cathodic background signal, this PEC biosensor could distinguish the effects of initial photocurrent and background noise, leading to a much more reliable analysis result. Under the optimal conditions, the PEC biosensor showed ultrasensitivity for CEA with a limit of detection down to 18.9 fg/mL and satisfactory selectivity. Based on the excellent anti-interferent ability and ultrasensitivity, the proposed PEC biosensing platform may show promising applications in early diagnosis of diseases and bioanalysis.

2. Experimental section

2.1. Materials and reagents

TiO_2 powder (P25) was purchased from the Degussa Co. (Germany). ITO electrode was purchased from Zhuhai Kaivo Electronic Components Co., Ltd (China). Carcinoembryonic antigen (CEA) was obtained from Shanghai Linc-Bio Science Co., Ltd, China. 6-mercaptohexanol (MCH), tris(2-carboxyethyl) phosphine hydrochloride (TCEP) and hydrogen tetrachloroaurate (III) trihydrate ($HAuCl_4 \cdot 3H_2O$, 99.999%) were obtained from Sigma Aldrich (USA). Sodium sulfide ($Na_2S \bullet 9H_2O$), ascorbic acid (AA), and cadmium nitrate ($Cd(NO_3)_2 \bullet 4H_2O$) were all offered by Sinopharm Chemical Reagent Co., Ltd. (China). Other chemicals were of analytical grade and used as received. All aqueous solutions were prepared with ultrapure water from a Milli-Q filtration system (Millipore Corp., USA). DNA oligonucleotide was acquired from Sangon Biotechnology Co., Ltd. and the sequence was listed in Table S1.

2.2. Apparatus

Transmission electron microscopy (TEM) image was characterized by JEM-2100F microscope (JEM-2100F, Japan). X-ray diffraction (XRD) experiment was carried out on an X-ray diffractometer (D/MAX-RA, Japan). The UV—vis spectrum was obtained using a DS5 UV—vis spectrophotometer (DS5, England). A Xe lamp (PLS-SXE300) fitted with a 420 nm filter was used as light source. PEC and electrochemical impedance spectroscopic (EIS) measurements were accomplished by a CHI 660E electrochemical workstation with a ITO electrode (diameter, 5.6 mm) as the working electrode, a saturated calomel electrode (SCE) as the reference electrode, and a platinum wire as the counter electrode. EIS measurements were performed in 0.1 M KCl +5 mM (1:1) $[Fe(CN)_6]^{3-/4-}$ solution in the frequency range from 0.1 Hz to 100 kHz with 5 mV as the amplitude.

2.3. Preparation of TiO_2@Au NPs

The TiO_2@Au NPs were successfully prepared as followed: 50 mg TiO_2 powders were injected into 50 mL of 0.01 wt% $HAuCl_4$ solution and stirred for 30 min. Subsequently, 500 μL of 1 mM AA solution was quickly added to the above solution for 60 min stirring. Then, the mixture was obtained and stored at 4 °C for further use.

2.4. Preparation of CdS QDs and signal probe

5.5 mL of Na_2S (0.1 M) aqueous solution was poured into 5 mL of $Cd(NO_3)_2$ (0.1 M) solution under stirring for 2 h. The synthetic

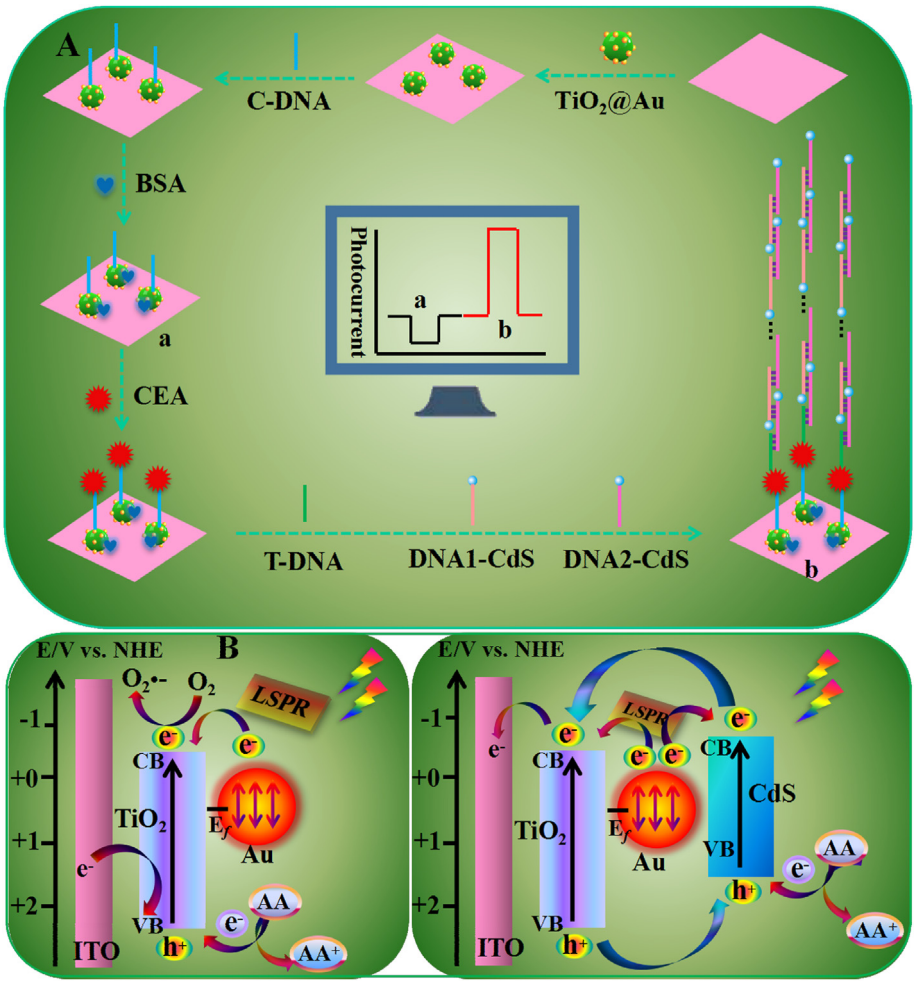

Scheme 1. (A) Schematic illustration for the preparation of PEC biosensor with cathodic background signal for CEA detection based on plasmonic TiO_2@Au NPs//CdS QDs photocurrent-direction switching system, (B) The photo-generated electron/hot transfer mechanism of TiO_2@Au and plasmonic TiO_2@Au NPs//CdS QDs system.

products were obtained by centrifugation and washing. Finally, the CdS QDs were scattered in 50 mL water. For the preparation of signal probe, 50 μL of 10 μM DNA probe 1 (DNA1) or DNA probe 2 (DNA2) were separately incubated with 1 mL of CdS QDs under gentle shaking for 12 h to achieve the signal probes (DNA1-CdS and DNA2-CdS).

2.5. Fabrication of the PEC biosensor and PEC assay

Prior to modification, ITO electrodes were cleaned by ultrasonic treatment for 15 min in acetone, 1 M NaOH in ethanol/water mixture (v/v, 1:1) and water, respectively, and then dried at 60 °C for 2 h. Then, 25 μL of the above TiO_2@Au NPs solution was dropped onto the ITO electrode surface, and the obtained electrode was labeled as ITO/TiO_2@Au electrode. Before assembled on the obtained electrode surface, the C-DNA was dissolved in PBS solution (20 mM, pH 7.4, 140 mM NaCl, 1 mM $MgCl_2$ and 10 mM TCEP), and incubated for 1 h to decrease disulfide bonds. Then, 20 μL of C-DNA solution (1.5 μM) was coated onto the surface of ITO/TiO_2@Au electrode at 4 °C for 12 h. The obtained ITO/TiO_2@Au/C-DNA electrode was immersed into 2 mM MCH for 1 h to prevent the non-specific adsorption. Next, the modified electrode was incubated with 20 μL PBS solution containing different-concentration CEA at 37 °C for 60 min to get ITO/TiO_2@Au/C-DNA/MCH/CEA electrode.

Before HCR reaction, DNA1-CdS and DNA2-CdS were separately incubated at 95 °C for 5 min and naturally cooled to room temperature. Afterwards, the mixture of T-DNA solution (2 μM), DNA1-CdS (2 μM) and DNA2-CdS (2 μM) was dropped onto the surface of resulted electrode and reacted for 90 min at 37 °C to form the HCR reaction. Finally, the PEC investigates were performed in Tris−HCl solution (0.1 M, pH 7.4) containing AA (0.1 M) at 0 V.

3. Results and discussion

3.1. Material characterization

The TEM was used for characterizing the as-synthesized TiO_2@Au NPs and the result was shown in Fig. 1A. The TiO_2@Au NPs are approximately 30 nm, and numerous Au NPs are coated on the surface of TiO_2 NPs, suggesting the successful preparation of TiO_2@Au NPs. The structural characteristic and crystalline phase analyses of TiO_2 and TiO_2@Au NPs were carried out by X-ray diffraction (XRD). As displayed in Fig. 1B, the characteristic peaks for TiO_2 at 25.6°, 38.1°, 48.3°, 54.2°, 55.3° and 63.1° correspond to the diffractions from the (101), (004), (200), (105), (211), and (204) planes of TiO_2 (JCPDS 21−1272). After the modification of Au NPs, some new peaks appear at 38.4°, 44.7°, 64.9° and 77.7° for TiO_2@Au composite, assigning to the diffractions of the (111), (200), (220), and (331) planes of Au. Furthermore, the UV−vis absorption spectra of TiO_2 and TiO_2@Au NPs were investigated (Fig. 1C). Compared

with bare TiO_2 NPs (curve a), the light absorption intensity of TiO_2@Au NPs (curve b) is significantly enhanced in the visible region, which indicates that Au NPs can enhance the adsorption behaviour of TiO_2 NPs [42]. However, no characteristic peak was detected for Au owing to its low volume fraction. As the Au content increases, an absorption peak at about 565 nm is coincident to that of the optical characteristic peak of Au NPs (Fig. S1) [23,40].

The obtained CdS QDs were observed by TEM and high resolution transmission electron microscopy (HRTEM). From Fig. 1D, the as-fabricated CdS QDs display a characteristic sphere-shape size distribution with 7 nm in diameter, and a interplanar distance of 0.292 nm matching with the (111) facet of CdS QDs [43,44]. The phase of CdS QDs are further characterized by XRD (Fig. 1E), and the peaks at 26.6°, 42.6° and 51.9° are determined, which assign to the diffractions of the (111), (220), and (311) planes from the CdS standard card (JCPDS No. 19−0191), respectively [45]. Moreover, the successful preparation of signal probes was confirmed by UV−vis absorption spectroscopy (Fig. 1F). It is noted that the DNA strands (DNA1 and DNA2) display inherent characteristic absorption peaks at 260 nm (curve a and b) [46]. Compared with CdS QDs which exhibit a broad light absorption from 540 nm to low wavelengths (curve c), the characteristic absorption of DNA is separately observed for DNA1-CdS (curve d) and DNA2-CdS (curve e), indicating that CdS QDs are successfully labeled on the DNA probes.

3.2. Characterization of the fabricated process of the PEC biosensor

EIS is an effective method for investigating the stepwise modified processes of the PEC biosensor. In Nyquist plot, the diameter of the semicircular circle represents the interfacial charge transfer resistance (R_{ct}) of an electrode. As described in Fig. 2A, the R_{ct} value of the ITO/TiO_2@Au electrode is 57.9 Ω (curve a). Subsequently, with the modifications order of C-DNA and MCH on the obtained electrode, the R_{ct} values are increased to 65.4 Ω (curve b) and 71.6 Ω (curve c), respectively, due to their blocking effect on the electron transfer process of the redox probe at the electrode. As showed in curve d, after the ITO/TiO_2@Au/C-DNA/MCH electrode captures target CEA, the R_{ct} value is enlarged (84.3 Ω). After further assembly with T-DNA, DNA1-CdS and DNA2-CdS, CdS is introduced to the biosensor based on the specific interaction between CEA and T-DNA, and the HCR is induced by T-DNA, DNA1 and DNA2, resulting in an increased R_{ct} value (109.7 Ω, curve e) due to the electrostatic repulsion action and steric hindrance resulting separately from DNA strands and CdS QDs. The obtained results demonstrate the successful fabrication of the biosensor.

To further confirm the successful construction of the PEC biosensing interface, PEC measurements were also performed (Fig. 2B). It is noted that the photocurrent decreases with the time during the light-on period due to the consumption of AA and O_2 [47]. Thus, the maximum photocurrent value is used throughout. The ITO/TiO_2@Au electrode shows an obvious cathodic background photocurrent (curve a), implying the good photoelectric conversion efficiency of TiO_2@Au NPs due to the LSPR-induced "hot electrons" transferring to the CB of the TiO_2 NPs and suppressing the photogenerated electrons/holes recombination of TiO_2. Subsequent successive introduction of C-DNA, MCH, and CEA on the surface of the ITO/TiO_2@Au electrode, the photocurrents successively decrease (curves b−d), which corresponds to the obtained EIS results (Fig. 2A). However, when the biosensor is incubated with the mixture of T-DNA, DNA1-CdS and DNA2-CdS bound by the HCR reaction, the plasmonic TiO_2@Au NPs//CdS QDs system is formed, leading to a switch of photocurrent direction and generation of the great anodic photocurrent (curve e). The presented results indicate that the proposed PEC biosensor with cathodic background signal can be employed for CEA detection.

3.3. Plasmonic TiO_2@Au NPs//CdS QDs photocurrent-direction switching mechanism

To confirm the superiority of TiO_2@Au NPs as the substrate photoactive material and CdS QDs as the switcher in this sensitive structure, some contrast experiments were characterized through comparing the photocurrent responses of the electrodes modified with different materials. In general, TiO_2-coated ITO electrode and TiO_2-coated ITO electrodes loaded with Au exhibit anodic photocurrent, which are typical for n-type semiconductors. However, different stimuli were implemented to switch the charge transport properties at electrode surfaces with semiconductor nanoparticles to yield switchable photocurrent direction, which included photonic, electrical, magnetic, thermal, pH, or chemical signals [36,37].

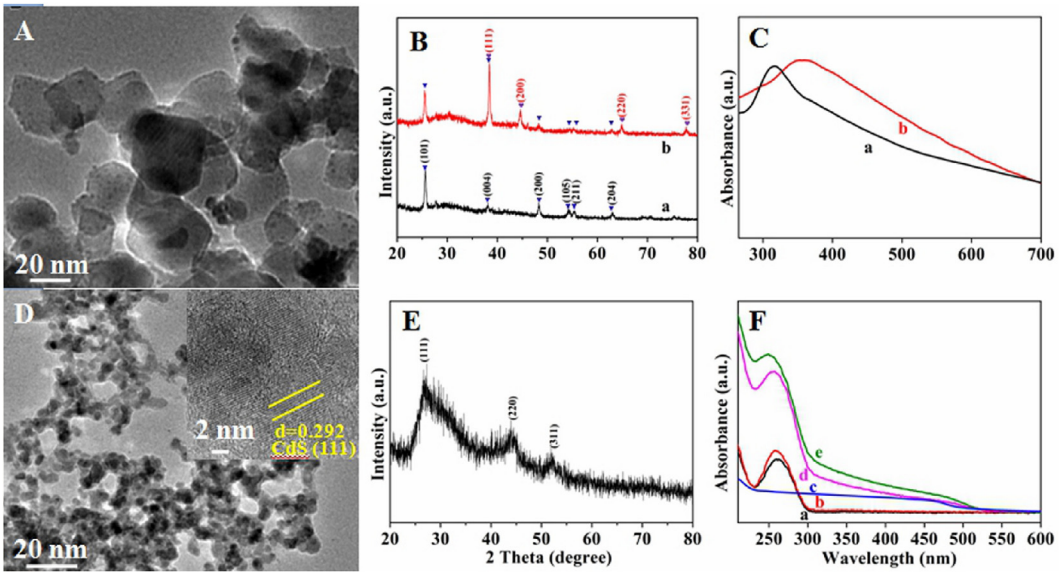

Fig. 1. (A) TEM image of TiO_2@Au NPs, (B) XRD patterns and (C) UV−vis absorption spectra of TiO_2 (a) and TiO_2@Au (b) NPs, (D) TEM image and (E) XRD pattern of CdS QDs, (F) UV−vis absorption spectra of DNA1 (a), DNA2 (b), CdS QDs (c), DNA1-CdS (d) and DNA2-CdS (e). Inset of D is the related HRTEM image of CdS QDs.

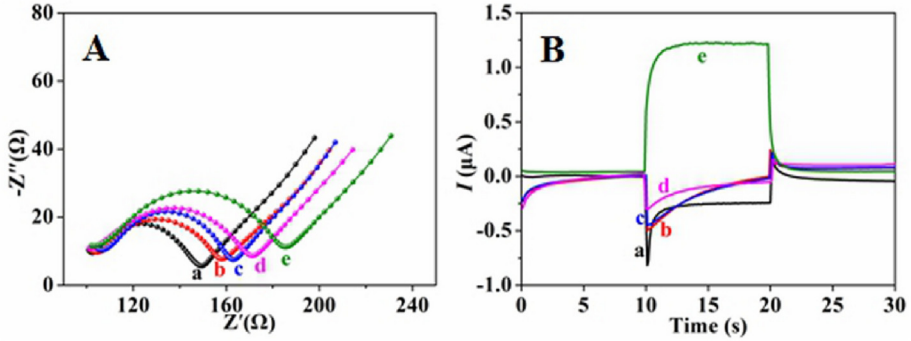

Fig. 2. (A) EIS results and (B) Photocurrent responses of (a) ITO/TiO_2@Au, (b) ITO/TiO_2@Au/C-DNA, (c) ITO/TiO_2@Au/C-DNA/MCH, (d) ITO/TiO_2@Au/C-DNA/MCH/CEA, (e) ITO/TiO_2@Au/C-DNA/MCH/CEA electrode after incubation with T-DNA + DNA1-CdS + DNA2-CdS.

As shown in Fig. 3A and B, the photocurrent response after modification of TiO_2 NPs on the bare ITO electrode is 2.211 μA, and the photocurrent of TiO_2@Au NPs-modified electrode is seen at about −0.826 μA. Comparison of Fig. 3A with 3B, it is noted that the as-prepared TiO_2@Au NPs in this work have benefits of cathodic background signal and high photoelectric efficiency in established PEC biosensor since the modification of Au NPs changes the photoelectric performance of TiO_2@Au NPs and the LSPR effect of plasmonic noble metal can reduce the electrons/holes recombination (Fig. S2) [38–41]. After the CEA-triggered the introduction of CdS QDs, the photocurrent direction of PEC biosensor is changed from cathodic to anodic photocurrents and the significant anodic photocurrents are obtained (3.593 μA, Fig. 3C), which is about 4.5 times bigger than that of TiO_2@Au NPs, on account of well-matched energy levels of TiO_2 NPs//CdS QDs, with large plasmonic enhancement and hot-electron injection mechanism of Au NPs. Additionally, the anodic photocurrent of DNA1-CdS + DNA2-CdS in Fig. 3C (3.593 μA) is larger than that of T-DNA-CdS in Fig. 3D (1.227 μA), because of the large amounts of CdS QDs introduced by HCR amplification strategy for enhancing anodic photocurrent. The above results manifest that CdS QDs as an ideal switcher can efficiently improve the photoelectric conversion efficiency of TiO_2@Au NPs to achieve amplification of the PEC responses.

To reveal the possible electron-transfer mechanism of plasmonic TiO_2@Au NPs//CdS QDs photocurrent-direction switching system, CB and VB of TiO_2 NPs and CdS QDs were investigated by electrochemical method (Fig. S3). The results show that TiO_2 NPs have a CB edge at −0.65 V and a VB edge at 2.12 V, and CdS QDs have a CB edge at −0.92 V and a VB edge at 1.34 V vs. SCE (equivalent to −0.41, 2.36, −0.68 and 1.58 V vs NHE, respectively.). These values will be useful for understanding the PEC behaviors of the designed TiO_2@Au NPs//CdS QDs system.

Based on the results shown in Fig. 3 and S3, a possible photocurrent generation mechanism of the TiO_2@Au NPs//CdS QDs system is illustrated in Scheme 1B. For the TiO_2@Au NPs, both TiO_2 and Au NPs can be excited under visible light illumination. The plasmon

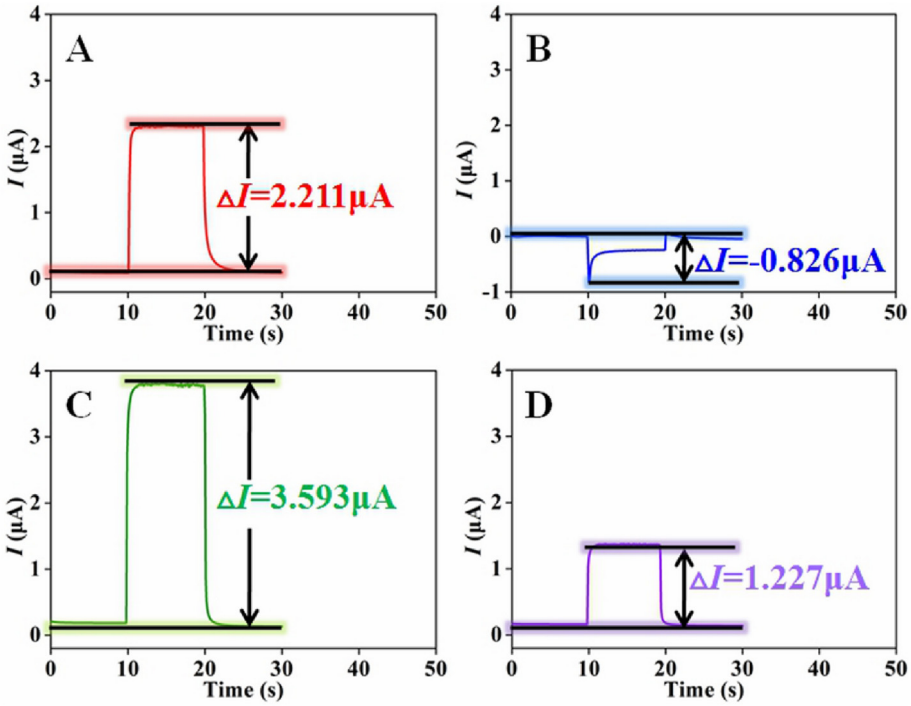

Fig. 3. PEC signal comparison of different modified electrodes: (A) ITO/TiO_2, (B) ITO/TiO_2@Au, (C) ITO/TiO_2@Au/C-DNA/MCH/CEA electrode after incubation with T-DNA + DNA1-CdS + DNA2-CdS, and (D) ITO/TiO_2@Au/C-DNA/MCH/CEA electrode after incubation with T-DNA-CdS.

resonance energy transfer promoted the photon absorption of TiO_2 NPs in the visible region with LSPR-induced localized electric field amplification, and the generated hot electrons by LSPR excitation in the Fermi level of Au were easily injected into CB of TiO_2 for the electrochemical reduction of O_2 (electron acceptors) in the electrolyte, leading to a cathodic photocurrent background [47–49]. After the introduction of CdS QDs, the well-matched energy bands between TiO_2 and CdS could make a significant contribution in the promotion of the separation and transfer of photo-generated electron/hole pairs. And the electrons on the CB of CdS (−0.68 eV vs NHE) moved to the CB of TiO_2 (−0.41 eV vs NHE), and finally transferred to the ITO electrode, thus generating the anodic photocurrent response. Additionally, the LSPR effect results in the generation of electron-hole pairs of Au NPs, and the hot electrons of Au NPs can be injected into the CB of TiO_2 and CdS, respectively, while Au NPs serve as the plasmonic photosensitizer for improving photocurrent response (Fig. S4) [50,51]. Besides, In order to clarify the influence of the applied potential on the working electrode on the PEC performance more clearly, the potential-dependent photocurrent toward different nanomaterials (TiO_2, TiO_2@Au NPs and TiO_2@Au NPs/CdS QDs) were investigated and 0 V is served as the optimal applied potential for this PEC biosensing (Figs. S5A–5C).

3.4. PEC detection of CEA

Under the optimal experimental conditions (Figs. S6A–6C), the analytical performance of the obtained PEC biosensing platform was characterized by incubating with different-concentration CEA and the results were showed in Fig. 4. From Fig. 4A, in the presence of CEA, a cathodic photocurrent background (I_0, -0.324 μA) of the electrode is changed from cathodic to anodic photocurrents, and the anodic photocurrent (I) enhances with the CEA increased concentration, which inferences that the proposed biosensor exhibits satisfactory analytical characteristics to eliminate false positive or negative errors, because the common interferences just decrease or increase cathodic photocurrents of the biosensor and not switch photocurrent direction from cathode to anode. The linear relationship between the value of photocurrent change ($\triangle I = I - I_0$) and CEA concentration is displayed in Fig. 4B. A linear response range of 0.2–20 pg/mL and a linear regression equation of $\triangle I\,(\mu A) = 0.2861 C_{CEA}\,(pg/mL) + 0.9458$ ($R^2 = 0.9984$) are achieved. The limit of detection is estimated to be 18.9 fg/mL (3σ). It can be seen that the fabricated PEC biosensor exhibits ultrahigh sensitivity with a lower detection limit than some previous reports (Table 1). Such improved sensitivity of this proposed PEC biosensor may be attributed to reasons as follows: (1) TiO_2@Au NPs exhibit cathodic background signal; (2) the well-matched energy levels between TiO_2@Au and CdS result in the high-efficiency photocurrent direction switching of the ITO/TiO_2@Au electrode; (3) large plasmonic enhancement and hot-electron injection mechanism of Au NPs can reduce the electrons/holes recombination; (4) HCR amplification strategy can introduce large amounts of CdS.

3.5. Selectivity, stability and reproducibility

Selectivity is a greatly significant parameter for the PEC biosensor. It was evaluated by several possible interfering proteins, such as alphafetoprotein (AFP), bovine serum albumin (BSA), IgG, CEA and prostatespecific antigen (PSA). From Fig. 5A, the photocurrent direction of the PEC biosensor is not changed by the interference and no obvious change of the anodic photocurrent response is surveyed compared with the blank. When target the CEA exists (5 pg/mL), the cathodic photocurrent of the prepared PEC biosensor is changed to an anodic photocurrent because of target CEA-induced the introduction of CdS QDs, leading to a photocurrent-direction switching. Additionally, the photocurrent responses towards only 5 pg/mL CEA is almost same with that towards the mixture of CEA (5 pg/mL) and other proteins (each 500 pg/mL), indicating that the prepared PEC biosensor possesses good selectivity.

The reproducibility of the developed biosensor was estimated, five parallel biosensors were utilized to analyze CEA (5 pg/mL), and the relative standard deviation (RSD) is 3.1%. In addition, the stability of the PEC biosensor was an important criterion for the application to bioassay. From Fig. 5B, no noticeable photocurrent change occurred in the PEC biosensor under off-on-off irradiation for 26 cycles. On the other hand, the storage stability of the biosensor was also evaluated during a 2-week period, by storing it at 4 °C in the refrigerator. The photocurrent response of the PEC biosensor toward CEA retained about 97.3% of its initial value. These results suggest that the prepared biosensor has good reproducibility and satisfactory stability.

3.6. CEA assay in human serum samples

To further study the feasibility and application potential, the prepared PEC biosensor was employed to detect CEA in sophisticated biological samples (collected from local affiliated hospital (Zhengzhou, China) according to the rules of the local ethical committee). Different-concentration CEA (0.2, 1, 5, 8 and 10 pg/mL) is added into 10-fold diluted serum samples (10 mM PBS, pH 7.4) for practical determination. As presented in Table 2, the average recoveries are from 96.7% to 103.5% with the RSDs of 1.2%–5.6%,

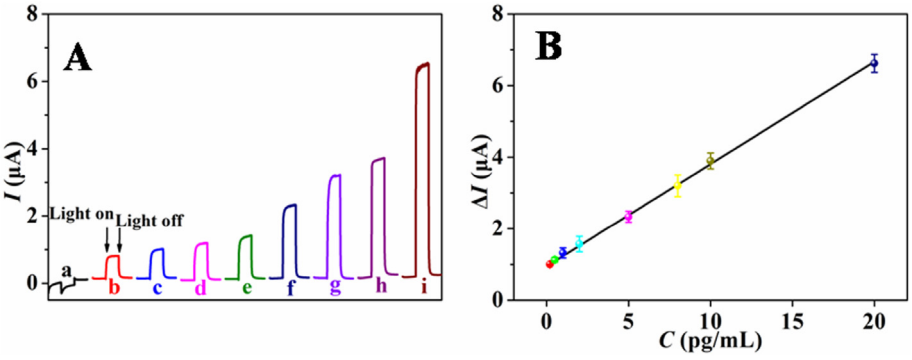

Fig. 4. (A) Photocurrent response of the biosensor with a series of CEA concentrations. The concentrations were (from a to i) 0, 0.2, 0.5, 1, 2, 5, 8, 10 and 20 pg/mL. (B) The calibration plot of I versus the CEA concentration.

Table 1
Comparison of various methods for CEA detection.

Method	Strategy	LOD	Ref.
quartz nanopipettes	Fe_3O_4@Au NPs	0.6 ng/mL	[52]
electrochemical	Ag/MoS_2@Fe_3O_4	30 fg/mL	[53]
fluorescent	CdTe/CdSe QDs	6.7 pg/mL	[54]
fluorescent	Exo III/DNA walker	1.2 pg/mL	[55]
electrochemiluminescence	g−C_3N_4−CNT@Au//CuO@PDA	25.7 fg/mL	[56]
electrochemiluminescence	CdTe//CdSe NCs	1 pg/mL	[57]
photoelectrochemical	SnS_2-GR//Au@CuS-GR	59.9 fg/mL	[32]
photoelectrochemical	g-C_3N_4/Au/Bi_2MoO_6	4.5 pg/mL	[50]
photoelectrochemical	$NaYF_4$:Yb,Er//Ag_2S	1.9 pg/mL	[31]
photoelectrochemical	TiO_2@Au NPs//CdS QDs	18.9 fg/mL	This work

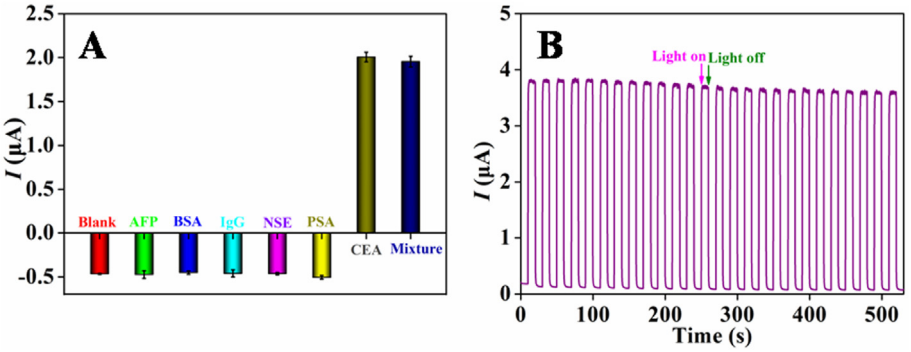

Fig. 5. (A) Selectivity of the biosensor. CEA (5 pg/mL), other proteins (AFP, BSA, IgG, NSE and PSA, each 500 pg/mL), and their mixture. (B) Time-dependent photocurrent signal of the PEC biosensor incubated with 10 pg/mL CEA for 26 on-off cycles.

demonstrating that the established PEC biosensor can possess great potential application and feasibility in human biological fluids.

4. Conclusions

Based on the innovative plasmonic TiO_2@Au NPs//CdS QDs photocurrent-direction switching system, an ultrasensitive and selective PEC biosensor was constructed for the detection of CEA coupling cathodic background signal with HCR for the signal amplification. After target CEA-induced HCR, abundant CdS QDs were introduced into the biosensing platform, resulting in the formation of TiO_2@Au NPs//CdS QDs system and the switch of the photocurrents from cathodic to anodic. The obtained remarkable anodic photocurrent was depended on the LSPR effect of Au between TiO_2 and CdS. The constructed PEC biosensor exhibited a linear range of 0.2−20 pg/mL with a low detection limit of 18.9 fg/mL. Importantly, this proposed biosensor could eliminate the interference caused by the varied initial current and background noise, and possessed high-efficiency anti-interference ability, satisfactory stability and excellent reproducibility. This design provides a universal PEC biosensing platform and has great potentials in bioanalysis and early diagnosis of disease.

Table 2
Recovery tests of CEA in the human serum sample.

Sample	Added (pg/mL)	Found (pg/mL)	RSD (%)	Recovery (%)
1	0.2	0.207	3.2	103.5
2	1	0.966	5.6	96.6
3	5	4.895	3.4	97.9
4	8	8.080	1.2	101.0
5	10	9.841	1.5	98.4

Declaration of competing interest

The authors declare that they have no known competing financial interests or personal relationships that could have appeared to influence the work reported in this paper.

Acknowledgements

This work was financially supported by the National Natural Science Foundation of China (No. 81973099) and China Postdoctoral Science Foundation (No. 2020M672259).

Appendix A. Supplementary data

Supplementary data to this article can be found online at https://doi.org/10.1016/j.aca.2021.338283.

References

[1] C.Q. Zhao, J. Zhou, K.W. Wu, S.N. Ding, J.J. Xu, H.Y. Chen, Plasmonic enhanced gold nanoclusters-based photoelectrochemical biosensor for sensitive alkaline phosphatase activity analysis, Anal. Chem. 92 (2020) 6886−6892.
[2] R.Y. Yang, K. Zou, Y.M. Li, L.X. Meng, X.H. Zhang, J.H. Chen, Co_3O_4-Au polyhedra: a multifunctional signal amplifier for sensitive photoelectrochemical assay, Anal. Chem. 90 (2018) 9480−9486.
[3] L.T. Huang, J.L. Chen, Z.H. Yu, D.P. Tang, Self-powered temperature sensor with seebeck effect transduction for photothermal−thermoelectric coupled immunoassay, Anal. Chem. 92 (2020) 2809−2814.
[4] D. Long, M.J. Li, H.H. Wang, H.J. Wang, Y.Q. Chai, R. Yuan, A photoelectrochemical biosensor based on fullerene with methylene blue as a sensitizer for ultrasensitive DNA detection, Biosens. Bioelectron. 142 (2019) 111579.
[5] C.C. Gu, P.P. Gai, X.K. Kong, T. Hou, F. Li, Self-powered biosensing platform based on "signal-on" enzymatic biofuel cell for DNA methyltransferase activity analysis and inhibitor screening, Anal. Chem. 92 (2020) 5426−5430.
[6] Y.X. Feng, T. Yan, T.T. Wu, N. Zhang, Q.Q. Yang, M. Sun, L.G. Yan, B. Du, Q. Wei, A label-free photoelectrochemical aptasensing platform base on plasmon Au coupling with MOF-derived In_2O_3@g-C_3N_4 nanoarchitectures for tetracycline

detection, Sens. Actuators, B 298 (2019) 126817.
[7] C.M. Gao, H.H. Yu, L.N. Zhang, Y.H. Zhao, J.X. Xie, C.J. Li, K. Cui, J.H. Yu, Ultrasensitive paper-based photoelectrochemical sensing platform enabled by the polar charge carriers-created electric field, Anal. Chem. 92 (2020) 2902–2906.
[8] Z.Z. Wang, J. Li, W.W. Tu, H.S. Wang, Z.Y. Wang, Z.H. Dai, Formation of a photoelectrochemical Z-scheme structure with inorganic/organic hybrid materials for evaluation of receptor protein expression on the membrane of cancer cells, ACS Appl. Mater. Interfaces 12 (2020) 26905–26913.
[9] C.C. Wang, Y. Li, E.S. Xu, Q. Zhou, J. Chen, W. Wei, Y. Liu, S.Q. Liu, A label-free PFP-based photoelectrochemical biosensor for highly sensitive detection of PARP-1 activity, Biosens. Bioelectron. 138 (2019) 111308.
[10] R.Y. Yang, K. Zou, X.H. Zhang, C.C. Du, J.H. Chen, Target-induced photocurrent-polarity switching: a highly selective and sensitive photoelectrochemical sensing platform, Chem. Commun. 55 (2019) 8939–8942.
[11] Q. Zhou, H.J. Xue, Y.Y. Zhang, Y.Q. Lv, H.G. Li, S.Q. Liu, Y.F. Shen, Y.J. Zhang, Metal-free all-carbon nanohybrid for ultrasensitive photoelectrochemical immunosensing of alpha-fetoprotein, ACS Sens. 3 (2018) 1385–1391.
[12] R.Y. Li, W.W. Tu, H.S. Wang, Z.H. Dai, Near-infrared light excited and localized surface plasmon resonance enhanced photoelectrochemical biosensing platform for cell analysis, Anal. Chem. 90 (2018) 9403–9409.
[13] N. Zhang, X.M. Shi, H.Q. Guo, X.Z. Zhao, W.W. Zhao, J.J. Xu, H.Y. Chen, J. Luo, L.C. Fang, H.M. Liu, Q.J. Zhu, H. Huang, J. Deng, F.X. Liu, Y. Li, J.S. Zheng, Gold nanoparticle couples with entropy-driven toehold-mediated DNA Strand displacement reaction on magnetic beads: toward ultrasensitive energy-transfer-based photoelectrochemical detection of miRNA-141 in real blood sample, Anal. Chem. 90 (2018) 11892–11898.
[14] F.Z. Chen, D.M. Han, H.Y. Chen, Liposome-assisted enzymatic modulation of plasmonic photoelectrochemistry for immunoassay, Anal. Chem. 92 (2020) 8450–8458.
[15] P.P. Liu, X.Q. Liu, X.H. Huo, Y.F. Tang, J. Xu, H.X. Ju, TiO_2–$BiVO_4$ heterostructure to enhance photoelectrochemical efficiency for sensitive aptasensing, ACS Appl. Mater. Interfaces 9 (2017) 27185–27192.
[16] B.B. Fan, Q. Fan, L.L. Hu, M. Cui, X.Y. Wang, H.M. Ma, Q. Wei, Polydopamine-PEG–folic acid conjugate film engineered TiO_2 nanotube arrays for photoelectrochemical sensing of folate binding protein, ACS Appl. Mater. Interfaces 12 (2020) 1877–1884.
[17] Y.L. Li, S.P. Zhang, H. Dai, Z.S. Hong, Y.Y. Lin, An enzyme-free photoelectrochemical sensing of concanavalin A based on graphene-supported TiO_2 mesocrystal, Sens. Actuators, B 232 (2016) 226–232.
[18] W.G. Ma, L.N. Wang, N. Zhang, D.X. Han, X.D. Dong, L. Niu, Biomolecule-free, selective detection of o-diphenol and its derivatives with WS_2/TiO_2-based photoelectrochemical platform, Anal. Chem. 87 (2015) 4844–4850.
[19] B. Wang, J.T. Cao, Y.X. Dong, F.R. Liu, X.L. Fu, S.W. Ren, S.H. Ma, Y.M. Liu, An in situ electron donor consumption strategy for photoelectrochemical biosensing of proteins based on ternary Bi_2S_3/Ag_2S/TiO_2 NT arrays, Chem. Commun. 54 (2018) 806–809.
[20] J. Zhu, X.H. Huo, X.Q. Liu, H.X. Ju, Gold nanoparticles deposited polyaniline–TiO_2 nanotube for surface plasmon resonance enhanced photoelectrochemical biosensing, ACS Appl. Mater. Interfaces 8 (2016) 341–349.
[21] L. Guo, H. Yin, M.L. Xu, Z.T. Zheng, X.H. Fang, R. Chong, Y.Y. Zhou, L.Q. Xu, Q. Xu, J. Li, H.B. Li, In situ generated plasmonic silver nanoparticle-sensitized amorphous titanium dioxide for ultrasensitive photoelectrochemical sensing of formaldehyde, ACS Sens. 4 (2019) 2724–2729.
[22] H.M. Deng, Y.C. Chai, R. Yuan, Y.L. Yuan, In situ formation of multifunctional DNA nanospheres for a sensitive and accurate dual-mode biosensor for photoelectrochemical and electrochemical assay, Anal. Chem. 92 (2020) 8364–8370.
[23] J. Shu, Z.L. Qiu, S.Z. Lv, K.Y. Zhang, D.P. Tang, Plasmonic enhancement coupling with defect-engineered TiO_{2-x}: a mode for sensitive photoelectrochemical biosensing, Anal. Chem. 90 (2018) 2425–2429.
[24] X.X. Yan, J.J. Li, R.Y. Yang, Y.M. Li, X.H. Zhang, J.H. Chen, A new photoelectrochemical aptasensor for prion assay based on cyclodextrin and Rhodamine B, Sens. Actuators, B 255 (2018) 2187–2193.
[25] Y.H. Zhang, M.J. Li, H.J. Wang, R. Yuan, S.P. Wei, Supersensitive photoelectrochemical aptasensor based on Br,N-codoped TiO_2 sensitized by quantum dots, Anal. Chem. 91 (2019) 10864–10869.
[26] Q.Z. Han, R.Y. Wang, B. Xing, T. Zhang, M.S. Khan, D. Wu, Q. Wei, Label-free photoelectrochemical immunoassay for CEA detection based on CdS sensitized WO_3@BiOI heterostructure nanocomposite, Biosens. Bioelectron. 99 (2018) 493–499.
[27] Y.Q. Chen, W.F. Deng, Y.M. Tan, Q.J. Xie, CdS quantum-dots-decorated V_2O_5 nanosheets as chemically etchable active materials for sensitive photoelectrochemical immunoassay of carcinoembryonic antigen, ACS Appl. Mater. Interfaces 12 (2020) 29066–29073.
[28] Q.F. Zhai, X.W. Zhang, Y. Xia, J. Li, E.K. Wang, Electrochromic sensing platform based on steric hindrance effects for CEA detection, Analyst 141 (2016) 3985–3988.
[29] H. Dai, S.P. Zhang, Z.S. Hong, Y.Y. Lin, A potentiometric addressable photoelectrochemical biosensor for sensitive detection of two biomarkers, Anal. Chem. 88 (2016) 9532–9538.
[30] G.M. Nie, Y. Tang, B. Zhang, Y. Wang, Q.F. Guo, Label-free photoelectrochemical immunosensing platform for detection of carcinoembryonic antigen through photoactive conducting poly(5-formylindole) nanocomposite, Biosens. Bioelectron. 116 (2018) 60–66.
[31] Z.L. Qiu, J. Shu, D.P. Tang, $NaYF_4$:Yb,Er upconversion nanotransducer with in-situ fabrication of Ag_2S for near-infrared light responsive photoelectrochemical biosensor, Anal. Chem. 90 (2018) 12214–12220.
[32] D. Huang, L. Wang, Y. Zhan, L.N. Zou, B.X. Ye, Photoelectrochemical biosensor for CEA detection based on SnS_2-GR with multiple quenching effects of Au@CuS-GR, Biosens. Bioelectron. 140 (2019) 111358.
[33] R.Y. Yang, K. Zou, X.H. Zhang, C.C. Du, J.H. Chen, A new photoelectrochemical immunosensor for ultrasensitive assay of prion protein based on hemin-induced photocurrent direction switching, Biosens. Bioelectron. 132 (2019) 55–61.
[34] R.Y. Yang, J. Liu, Sensitive and selective photoelectrochemical immunosensing platform based on potential-induced photocurrent-direction switching strategy and a direct Z-scheme CdS//hemin photocurrent-direction switching system, J. Electroanal. Chem. 873 (2020) 114346.
[35] W.C. Geng, R.Y. Yang, A triple-helix molecular switch photoelectrochemical biosensor for ultrasensitive microRNA detection based on position controllable CdS//CdTe signal enhancement and switching, Chem. Commun. 56 (2020) 2909–2912.
[36] A. Efrati, O. Yehezkeli, R. Tel-Vered, D. Michaeli, R. Nechushtai, I. Willner, Electrochemical switching of photoelectrochemical processes at CdS QDs and photosystem I-modified electrodes, ACS Nano 6 (2012) 9258–9266.
[37] S. Yasutomi, T. Morita, S. Kimura, pH-controlled switching of photocurrent direction by self-assembled monolayer of helical peptides, J. Am. Chem. Soc. 127 (2005) 14564–14565.
[38] Photocurrent switching of monolayer MoS2 using a metal–insulatorn transition J.H. Lee, H.Z. Gul, H. Kim, B.H. Moon, S. Adhikari, J.H. Kim, H. Choi, Y.H. Lee, S.C. Lim, Nano Lett. 17 (2017) 673–678.
[39] M.F. Oszajca, K.L. McCall, N. Robertson, K. Szacizowski, Photocurrent switching effects in TiO2 modified with ruthenium polypyridine complexes, J. Phys. Chem. C 115 (2011) 12187–12195.
[40] N. Sakai, Y. Fujiwara, Y. Takahashi, T. Tatsuma, Plasmon-resonance-based generation of cathodic photocurrent at electrodeposited gold nanoparticles coated with TiO_2 films, ChemPhysChem 10 (2009) 766–769.
[41] H.J. Chen, G. Liu, L.Z. Wang, Switched photocurrent direction in Au/TiO_2 bilayer thin films, Sci. Rep. 5 (2015) 10852.
[42] W.C. Geng, D.L. Li, J.L. Sang, L.L. Pan, Z.L. Jiang, C. Liu, Y.J. Li, Engineering one-dimensional trough-like Au–Ag_2S nano-hybrids for plasmon-enhanced photo electrodetection of human α-thrombin, J. Mater. Chem. B 8 (2020) 10346–10352.
[43] J.T. Cao, Y. Ma, J.L. Lv, S.W. Ren, Y.M. Liu, A potentiometric resolved photoelectrochemical system based on CdS nanowires and $SnNb_2O_6$ nanosheets: a case application for dual biomarker analysis, Chem. Commun. 56 (2020) 1513–1516.
[44] J.T. Cao, Y.X. Dong, Y. Ma, B. Wang, S.H. Ma, Y.M. Liu, A ternary CdS@Au-g-C_3N_4 heterojunction-based photoelectrochemical immunosensor for prostate specific antigen detection using graphene oxide-CuS as tags for signal amplification, Anal. Chim. Acta 1106 (2020) 183–190.
[45] Y.X. Dong, J.T. Cao, B. Wang, S.H. Ma, Y.M. Liu, Spatial-resolved photoelectrochemical biosensing array based on a CdS@g-C_3N_4 heterojunction: a universal Immunosensing platform for accurate detection, ACS Appl. Mater. Interfaces 10 (2018) 3723–3731.
[46] Z.Y. Ma, F. Xu, Y. Qin, W.W. Zhao, J.J. Xu, H.Y. Chen, Invoking direct exciton–plasmon interactions by catalytic Ag deposition on Au nanoparticles: photoelectrochemical bioanalysis with high efficiency, Anal. Chem. 88 (2016) 4183–4187.
[47] R.Y. Yang, Y.M. Li, K. Zou, L.X. Meng, X.H. Zhang, J.H. Chen, A label-free and blocker-free photoelectrochemical strategy for highly sensitive caspase-3 assay, Chem. Commun. 54 (2018) 4830–4833.
[48] R.Y. Yang, X.X. Yan, Y.M. Li, X.H. Zhang, J.H. Chen, Nitrogen-doped porous carbon-ZnO nanopolyhedra derived from ZIF-8: new materials for photoelectrochemical biosensors, ACS Appl. Mater. Interfaces 9 (2017) 42482–42491.
[49] G.Y. Zhang, Y.H. Zhuang, D. Shan, G.F. Su, S. Cosnier, X.J. Zhang, Zirconium-based porphyrinic metal–organic framework (PCN-222): enhanced photoelectrochemical response and its application for label-Free phosphoprotein detection, Anal. Chem. 88 (2016) 11207–11212.
[50] Z.L. Qiu, J. Shu, D.P. Tang, Plasmonic resonance enhanced photoelectrochemical aptasensors based on g-C_3N_4/Bi_2MoO_6, Chem. Commun. 54 (2018) 7199–7202.
[51] T.T. Wu, T. Yan, X. Zhang, Y.X. Feng, D. Wei, M. Sun, B. Du, Q. Wei, A competitive photoelectrochemical immunosensor for the detection of diethylstilbestrol based on an Au/UiO-66(NH_2)/CdS matrix and a direct Z-scheme Melem/CdTe heterojunction as labels, Biosens. Bioelectron. 117 (2018) 575–582.
[52] H.R. Tang, H. Wang, C. Yang, D.D. Zhao, Y.Y. Qian, Y.X. Li, Nanopore-based strategy for selective detection of single carcinoembryonic antigen (CEA) molecules, Anal. Chem. 92 (2020) 3042–3049.
[53] Y.G. Wang, G.H. Zhao, Y. Zhang, X.H. Pang, W. Cao, B. Du, Q. Wei, Sandwich-type electrochemical immunosensor for CEA detection based on Ag/MoS_2@Fe_3O_4 and an analogous ELISA method with total internal reflection microscopy, Sens. Actuators, B 266 (2018) 561–569.
[54] Z.L. Qiu, J. Shu, D.P. Tang, Bioresponsive release system for visual fluorescence detection of carcinoembryonic antigen from mesoporous silica nanocontainers mediated optical color on quantum dot-enzyme-impregnated paper, Anal. Chem. 89 (2017) 5152–5160.
[55] M.Q. He, K. Wang, W.J. Wang, Y.L. Yu, J.H. Wang, Smart DNA machine for

carcinoembryonic antigen detection by exonuclease III-assisted target recycling and DNA walker cascade amplification, Anal. Chem. 89 (2017) 9292–9298.
[56] C. Song, X.J. Li, L.H. Hu, T.F. Shi, D. Wu, H.M. Ma, Y. Zhang, D.W. Fan, Q. Wei, H.X. Ju, Quench-type electrochemiluminescence immunosensor based on resonance energy transfer from carbon nanotubes and Au nanoparticles-enhanced g-C_3N_4 to CuO@polydopamine for procalcitonin detection, ACS Appl. Mater. Interfaces 12 (2020) 8006–8015.
[57] J. Zhou, L. Nie, B. Zhang, G.Z. Zou, Spectrum-resolved triplex-color electrochemiluminescence multiplexing Immunoassay with highly-passivated nanocrystals as tags, Anal. Chem. 90 (2018) 12361–12365.

Ruiying Yang is currently a associate professor at College of Public Health, Zhengzhou University, China. Her research interests focus on the design and development of photoelectrochemical biosensor for detection and bioanalysis.

Guihua Jiang is currently a master candidate at College of Chemistry and Molecular Engineering, Zhengzhou University, China. Her research interests focus on the photoelectrochemical detection of biomolecules.

Jie Liu is currently a senior laboratory technician at College of Public Health, Zhengzhou University, China. Her research interests focus on developing photoelectrochemical probes.

Yilin Wang is currently a lecturer at College of Public Health, Zhengzhou University, China. His research interests focus on developing fluorescent probes.

Ningge Jian is currently a lecturer at College of Public Health, Zhengzhou University, China. His research interests focus on developing fluorescent probes.

Leiliang He is currently a associate professor at College of Public Health, Zhengzhou University, China. His research interests focus on developing nanoprobes for bioanalysis.

Li'e Liu is currently a professor at College of Public Health, Zhengzhou University, China. Her research interests focus on developing fluorescent probes and food safety monitoring.

Lingbo Qu is currently a professor at College of Chemistry and Molecular Engineering, Zhengzhou University, China. His research interests focus on food safety monitoring and biosensors.

Yongjun Wu is currently a professor at College of Public Health, Zhengzhou University, China. His research interests focus on food safety monitoring and rapid detection technology.